



Effects of cathode materials on H₂O₂ production in microbial fuel cells

Pin-Hsueh Wu^a, Yinhan Wang^b, Pei-Hsun Wu^a, Shih-Yuan Lu^c, Chang-Ping Yu^{a,*}

^aGraduate Institute of Environmental Engineering, National Taiwan University, Taipei 10617, Taiwan, Tel. +886-2-3366-3729, email: cpyu@ntu.edu.tw (C.-P. Yu)

^bXiamen Institute of Rare-earth Materials, Haixi Institutes, Chinese Academy of Sciences, Xiamen, Fujian 361021, China

^cDepartment of Chemical Engineering, National Tsing Hua University, Hsinchu30013, Taiwan

Received 5 June 2018; Accepted 3 March 2019

ABSTRACT

The application of microbial fuel cells (MFCs) on wastewater treatment has been evolving rapidly in recent years. It provides simultaneous pollutants removal as well as energy recovery in treating wastewater. MFCs can also be needed to produce H₂O₂ and drive electro-Fenton reaction to remove emerging contaminants in wastewater. However, the cell voltage produced in a MFC is lower than the voltage used to drive the conventional electro-Fenton system. Therefore, this study intended to explore the H₂O₂ formation reactions on the cathode materials of the conventional electro-Fenton system in the MFC. In this study, H₂O₂ production kinetics on different cathode materials, including the non-catalytic materials such as graphite and steel plate, the high specific surface area materials such as carbon nanotubes, activated carbon, the catalytic materials such as platinum-titanium plate and the high specific surface area catalytic materials such as manganese oxide/carbon aerogel were evaluated. These cathode materials showed different H₂O₂ production performance. Among them, the manganese oxide/carbon aerogel with high specific surface area and catalytic activity demonstrated the best performance of H₂O₂ production among testing materials. The reaction kinetics of H₂O₂ production rates on high specific surface area cathode materials, the activated carbon and carbon nanotubes, were found to be pseudo-first order. However, for the cathode materials with catalytic surface, the manganese oxide/carbon aerogel and platinum titanium, the reaction kinetics of H₂O₂ production rates were found to be pseudo-zero order within 12 h. Our results suggest that the catalytic cathode materials with high specific surface area, like manganese oxide/carbon aerogel, may be more promising for H₂O₂ production in MFCs to provide the electro-Fenton system. Therefore, the development of better cathode materials should be focused for the future application of MFCs driven electro-Fenton system.

Keywords: Microbial fuel cells (MFCs); Hydrogen peroxide; High specific surface area materials; Catalytic materials; Kinetics

1. Introduction

Most of the current sewage treatment processes have high energy consumption. The energy consumption of wastewater treatment accounted for about 3% of total energy use in the United States [1], equivalent to 15 GW. With electricity prices continuing to rise, energy recovery from sewage treatment becomes important strategy for water treatment projects. Liu and Logan [2] estimated the total wastewater in the USA, including domestic wastewa-

ter, industrial wastewater and livestock wastewater, had an energy potential of 17 GW, exceeding the energy consumption required for treatment.

Using microbial fuel cells (MFCs) to harvest the energy from wastewater treatment has been evolving rapidly in recent years. Utilizing the anodic microorganisms to oxidize organic matter in the wastewater, MFCs can remove pollutants and recover energy at the same time [3]. In general, there are two different MFC designs, the dual-chamber and single-chamber MFCs (Fig. 1). In the dual-chamber MFC (Fig. 1a) [4], the microorganisms grown on the anode metabolize the organic matter into carbon dioxide and H⁺

*Corresponding author.

and release electrons to anode (Thus electricity can be produced in the external electrons flow). The generated H^+ will be transported through the proton exchange membrane onto the cathode surface where it reacts with the dissolved oxygen and electrons to produce water. In the single-chamber MFC (Fig. 1b), the cathode is exposed to air, which allows the oxygen in the air to directly react with H^+ and the electrons. The single-chamber MFC reduces energy consumption for aeration, but it is more difficult to synthesize valuable byproducts in the cathodic chamber [4].

The low potential gradient generated in the MFC, due to high over potentials on the electrode materials, was commonly one of the hurdles to recover energy efficiently. Beside the direct use of the electric energy, MFCs were also demonstrated to produce valuable byproducts such as hydrogen and methane in the cathodic chamber [4]. Studies have also demonstrated carbon capture and disinfectant production in the cathode of MFCs [5,6]. In addition, by reducing the external resistance of MFCs, H_2O_2 concentration generated at the cathode could exceed the threshold level to drive the electro-Fenton reaction, which provided a strong oxidant to degrade pollutants [7,8]. The electro-Fenton reaction occurs by electrolysis of water molecules that generates hydrogen peroxide and hydrogen ions for classic Fenton reaction [9]. A standard electro-Fenton system has electrolysis of water occurring at the anode, and the H_2O_2 generated at the cathode. In the MFC driven electro-Fenton system, the anode is used for microbial reactions that generate electrons and

H^+ . The production of H_2O_2 and subsequent Fenton reaction take place in the cathodic chamber. Using smaller external resistors will result in higher current to enhance H_2O_2 production in the cathode [8,10]. The anodic and cathodic chambers are separated by a proton exchange membrane. Therefore, the microbial activity will not be influenced by the produced H_2O_2 or subsequent Fenton reaction when ferrous ion is provided.

In this study, dual-chamber MFCs were used to investigate the H_2O_2 production reaction using the cathode materials reported in most of electro-Fenton systems reported, such as steel plate [11], platinum titanium [12], graphite [13], activated carbon [14], carbon nanotubes [15] and newly synthesized material manganese oxide/carbon aerogel [16]. These cathodes consisted of non-catalytic materials, high specific surface area materials, catalytic materials as well as high specific surface area catalytic materials. In this study, the performance and reaction kinetics of H_2O_2 production in the cathode under low voltage conditions in MFCs was investigated in order to facilitate the selection of cathode materials to utilize the H_2O_2 produced in MFCs effectively.

2. Materials and methods

2.1. MFC configuration and operation

Dual-chamber MFCs made of acrylic plastic material consisting of the cathodic and anodic chambers were used. Both chambers have a square structure of $5 \times 5 \times 5$ cm, and are separated by a proton exchange membrane (Zhejiang Qianqiu Co., Hangzhou, China). Two graphite rods (8 cm long with a radius of 0.5 cm) and 100 pieces of graphite granules (0.6 cm height with a radius of 0.25 cm) (Qianqiu, Zhejiang, China) were initially used for both the anode and cathode as reported in previous study [8] for a base line of H_2O_2 production. In later experiments, different cathode materials were evaluated to compare the H_2O_2 production.

Solution in the anode chamber contained glucose (12 mM), NH_4Cl (2 mM), KCl (5 mM), $Na_2HPO_4 \cdot 12H_2O$ (0.2 M), and $NaH_2PO_4 \cdot 2H_2O$ (0.2 M), and the pH was adjusted to 7.0 ± 0.1 by $NaOH$, measured by a pH meter (Denver instrument UB-7, US). The solution in cathode chamber contained 14.2 g L^{-1} Na_2SO_4 solution, and was adjusted to $pH 3 \pm 0.1$ and aerated to produce H_2O_2 similar to the conditions reported in Wang et al. [8]. The MFCs was operated in batch mode and anode solution was changed every 2 d during enrichment but was changed every day when doing H_2O_2 production experiments. The inoculum in this study was collected from rice paddy soil of our laboratory-scale plant (rice) MFCs, which have been run for more than 3 months (data not shown). Three hundred grams of rice paddy soil was mixed in 1 L of water, and 100 mL of the mixed liquid was added into the anode chamber of MFCs. H_2O_2 production was measured when the cell voltage was stable with 10Ω resistor loaded in the external circuit. The H_2O_2 samples were collected at 0, 4, 6, 8, 10, 12 and 24 h after the start of the experiment. All experiments were conducted in duplicate.

2.2. Cathode materials

The cathode materials used in this study have mostly been reported for electro-Fenton reaction. The specific sur-

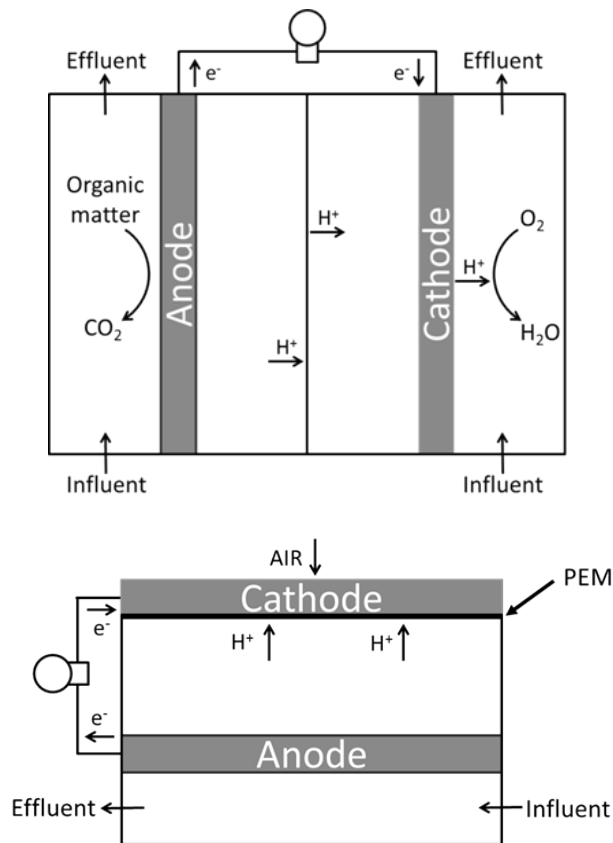


Fig. 1. Microbial fuel cell structures (a) dual chambers; (b) single chamber.

face area of “the high specific surface area” cathode materials are as follows: Activated carbon $900 \text{ m}^2 \text{ g}^{-1}$ (prepared from firewoods as described in Wu et al. [17]), carbon nanotubes $450 \text{ m}^2 \text{ g}^{-1}$ (S-MWCNT8, Conjutek, Taiwan), manganese oxide/carbon aerogel $577 \text{ m}^2 \text{ g}^{-1}$. The thickness of the steel plate and platinum titanium is 0.1 cm (Guang Yi Electrochemical Equipment, Taiwan).

Each testing cathode material was made into six 10 cm long and 1 cm wide plate electrode. The activated carbon, carbon nanotubes, manganese oxide/carbon aerogel, were pasted on a 0.5 cm thick graphite plate (Flying Carbon Enterprise Co., Taiwan) using conductive adhesive (polyvinylidene difluoride). These particles pasted electrode were prepared by 1) mixing material powders into polyvinylidene difluoride binders (2 wt.%) for 30 min; 2) adding N-methyl-2-pyrrolidone into the mixture before smeared onto the graphite plate; 3) dried in a vacuum oven at 50°C overnight [17].

The manganese oxide/carbon aerogel in this study was synthesized by sol-gel method [16]. In this procedure, 0.035 g sodium carbonate and 26.4 g resorcinol were dissolved in 34.735 mL deionized water and mixed with 35 mL methanol. The preliminary polymerization took 90 min when the solution was turned yellowish. Solution was incubated for one day at room temperature and put into 50°C oven for another day till the solution turned into a dark brownish gel. The gel was incubated for 5 d before daily immerses and rinsed with 200 proof ethanol for 4 d. The gel was carbonized with N_2 in 1000°C for 8 h to get the carbon aerogel. Potentiostatic method was used to deposit Mn_3O_4 at 1.5 V for 580 s, to make a composite of manganese oxide/carbon aerogel.

2.3. Analytical methods

H_2O_2 content was measured by the colorimetric method. Solution A contained 66 g L^{-1} KI, 2 g L^{-1} NaOH, 0.2 g L^{-1} ammonium molybdate, and was stored in a brown bottle. Solution B contained 20 g L^{-1} potassium hydrogen phthalate. 3 mL sample was mixed with 1 mL solution B before 1 mL solution A was added in the dark. The solution was analyzed at the wavelength of 351 nm in a spectrophotometer (Metash UV-5200 Spectrophotometer, China). The COD was analyzed by the COD measurement system with reagent kit (Lianhua Technology, Beijing, China). Specific surface area of electrode was determined from nitrogen adsorption data at 77K, $P/P_0 = 0.99$ using the BET-Sorptometer (BET-201A, Porous Materials Inc.). Voltage is continuously monitored every 10 min by data acquisition system (USB7660-B, ZTIC, China). Power density is calculated according to $P = 10 \times V^2 / (R \times A)$, where P is the power density (mW m^{-2}), V (mV) is the measured voltage, R (Ω) is the external resistance, and A (cm^2) is the electrode area.

3. Results and discussion

3.1. Degradation of organic matter in the anodic chamber

In the study, initial COD of 1200 mg L^{-1} was provided into the MFCs to avoid insufficient COD that would limit microbial activity in the anode and indirectly prevented the production of H_2O_2 in the cathode. It was observed that COD could drop to 60% from initial level after 48 h in the

anodic chamber when the MFC systems reached steady state. We observed the similar COD degradation trend irrelevant to cathode materials. Fig. 2 shows the typical COD degradation curve with graphite rod electrodes. The COD degradation rate gradually decreased; 50% COD reduced after 24 h and 60% dropped at 48 h. All H_2O_2 production experiments were completed within 24 h. Therefore, there would be no effect of the limitation of COD concentration in the anodic chamber on H_2O_2 production in the cathode.

3.2. Current generation

In the experiment, a 10Ω resistor was used as the external resistor in MFCs, and voltages generated by the microbial anode were recorded for different cathode materials. The average voltage of carbon-based cathode materials, including graphite, activated carbon, carbon nanotubes and manganese oxide/carbon aerogel was in the range of 30–40 mV, resulting in the current of 3.3–4.4 mA within 24 h (Fig. 3). The graphite cathode MFC had the maximum power density of 39 mW/cm^2 and internal resistance of $1.4 \text{ K}\Omega$ (Fig. 4). The metallic material, platinum titanium cathode, had voltage in the range of 25–30 mV, i.e. current of 2.5–3 mA, slightly lower than carbon-based materials (Fig. 3). The current from steel plate was the lowest, which is similar to the study in Behera et al. [18]. Replenishing the anode solution would cause the increase of voltage amplitude before it slowly decreased, which was also observed by Wang et al. [8].

3.3. pH change

The pH change in the cathodic chamber is shown in Fig. 5. As shown in Fig. 5, H^+ consumption in the initial stage of the reaction was very rapid but gradually decreased. Cathode materials of platinum titanium, activated carbon, carbon nanotubes, manganese oxide/carbon aerogel and graphite consumed H^+ in the cathodic chamber and resulted in solution pH 10 within 10 h. High specific surface area cathode materials such as activated carbon, carbon nanotubes and manganese oxide/carbon aerogel consumed H^+ faster, and within 6 h the solution reached the pH 10 and

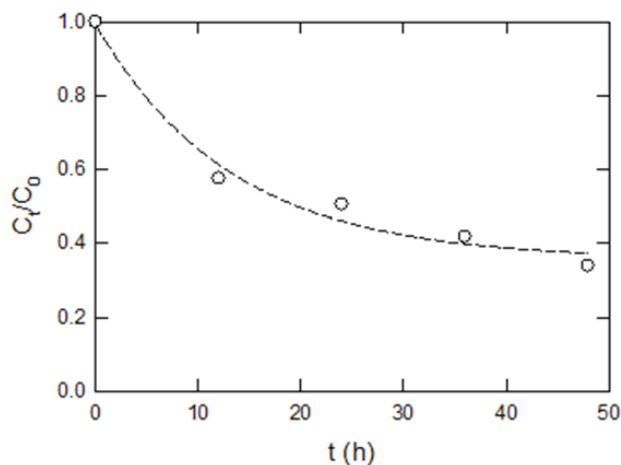


Fig. 2. COD degradation in the anodic chamber of microbial fuel cells with graphite rod cathodes.

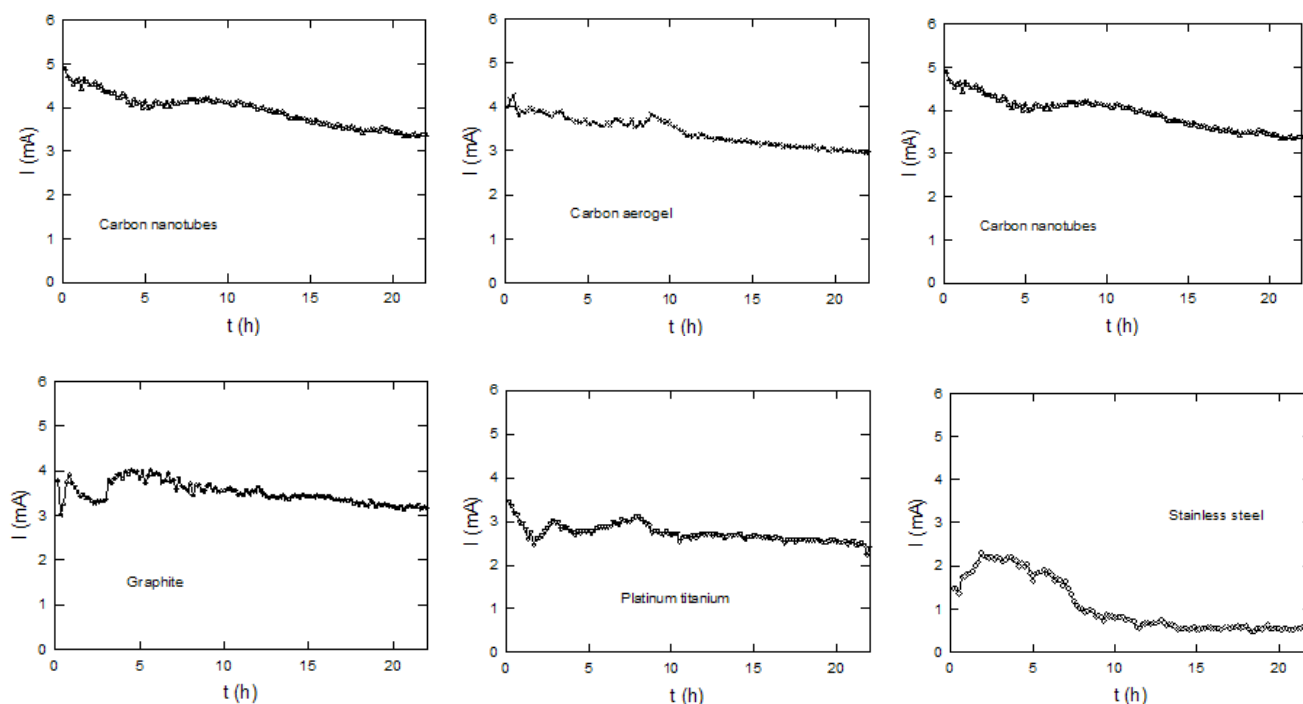


Fig. 3. Electric current output using the $10\ \Omega$ external resistor with different cathode materials.

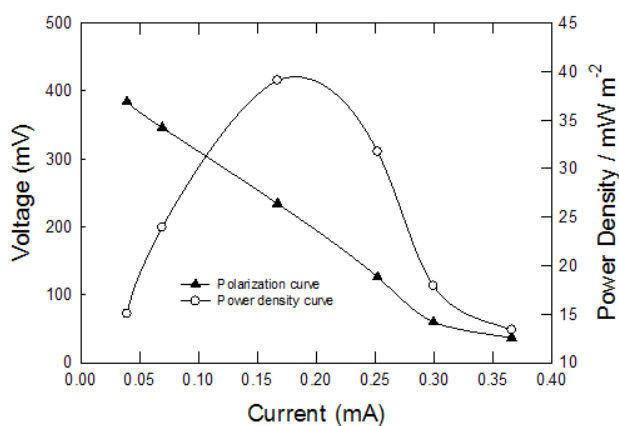


Fig. 4. Power density curve and polarization curve for the MFC with graphite rod electrodes.

remained constant. Low specific surface area materials like platinum-titanium and graphite consumed H^+ very slow that the solution pH reached 10 around 10–12 h. The constant pH at 10 implied that the cathodic reaction could possibly reach equilibrium. When steel plate cathode material was used, however, the pH in the cathodic chamber only slowly increased to 5 after 24 h. This slow consumption of H^+ was in accordance with the lower current production by the steel plate cathode shown in Fig. 3.

3.4. H_2O_2 synthesis

In this study, we used two MFC reactors as replicates, and examined the characteristics of the H_2O_2 production

for each cathode material. The H_2O_2 synthesis profile using graphite rods cathode was consistent with the previous research [8]. The generation of H_2O_2 reached maximum value between 4–8 h, and then gradually declined. According to Fromherz et al. [19], the carbon atoms on the graphite surface had an affinity for H^+ and O_2 to assist H_2O_2 synthesis. However, the reaction speed for graphite cathode was not fast enough to maintain the concentration of H_2O_2 when pH increased in the cathodic chamber. The rise of OH^- concentrations in water would increase the self-degradation reaction of H_2O_2 [8,20]. Since H_2O_2 generation could not keep up with its degradation, total H_2O_2 concentration decreased to $2\ mg\ L^{-1}$ at 12 h and $1.2\ mg\ L^{-1}$ at 24 h (Fig. 6). When using steel plate cathode, the production of H_2O_2 dropped to $0.6\ mg\ L^{-1}$, likely due to the higher cathodic over potential on electrode surface that resulted in the decrease of electromotive force (the cell voltage), which was also reflected by the slow H^+ consumption. Using catalytic cathode material, platinum-coated titanium, since the platinum will trap the oxygen atoms to form Pt-OO [21] that may facilitate (or catalyze) the oxygen and H^+ reaction to form H_2O_2 . Its H_2O_2 generation rate was higher and the maximum H_2O_2 concentration reached $9.4\ mg\ L^{-1}$, 3.76 times higher than produced on graphite rods cathode. Comparing the H_2O_2 production per unit electrode surface area in cm^2 , platinum titanium cathode produced 56 times higher H_2O_2 than graphite rods cathode (Table 1).

The H_2O_2 generation on the high specific surface area cathode materials was much higher than graphite rods cathode. The maximum H_2O_2 concentrations were $29\ mg\ L^{-1}$ and $31\ mg\ L^{-1}$, respectively using activated carbon and carbon nanotubes, which was around 11 times higher than that of graphite rods cathode. When considering the H_2O_2 production per unit electrode surface area, the H_2O_2 pro-

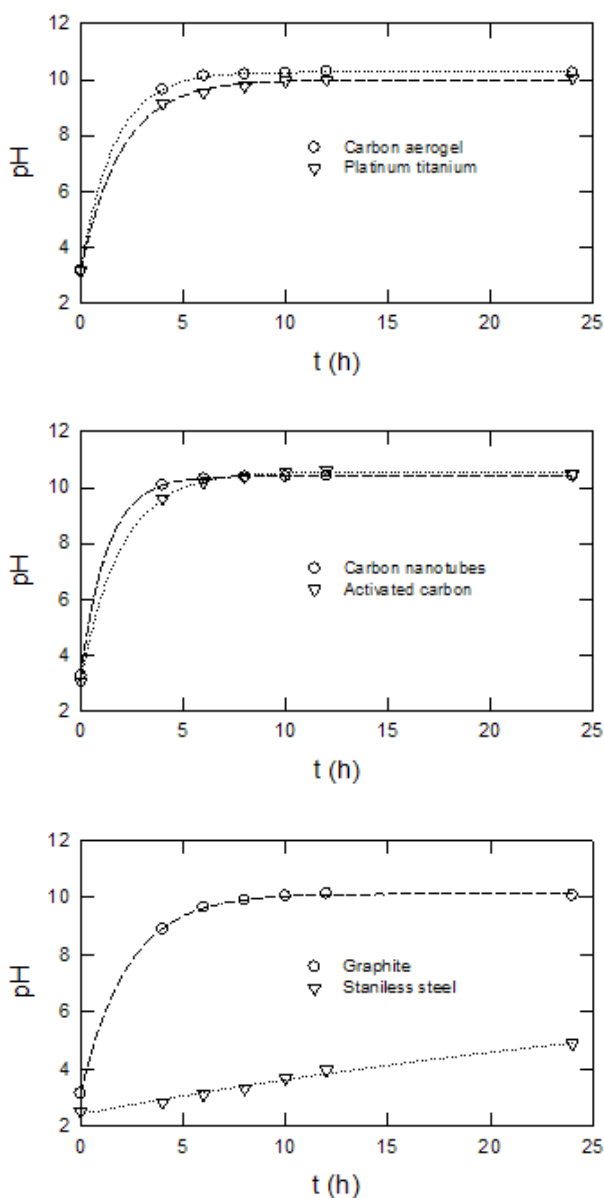


Fig. 5. pH change in the cathodic chamber with different cathode materials while H_2O_2 was produced.

duction was nearly 200 times higher than that of graphite rods cathode. This may be due to both the effects of high reaction surface and the higher specific surface area materials that can activate the adsorption of H^+ and oxygen atoms for reaction to form H_2O_2 . Therefore, the rate of initial reaction increased. Although the increase of pH in the cathodic chamber would trigger the self-degradation reaction of H_2O_2 , the higher specific surface area materials could have sufficient reaction surfaces to maintain H_2O_2 concentration.

Manganese oxide/carbon aerogel cathode, which had high specific surface area and catalytic properties, showed the highest H_2O_2 production of 40 mg L^{-1} . According to the previous research [22], the manganese oxide surface would capture H^+ to form $MnO\text{-OH}$ and would combine with water to form $MnOOH$ [23], which could be helpful for

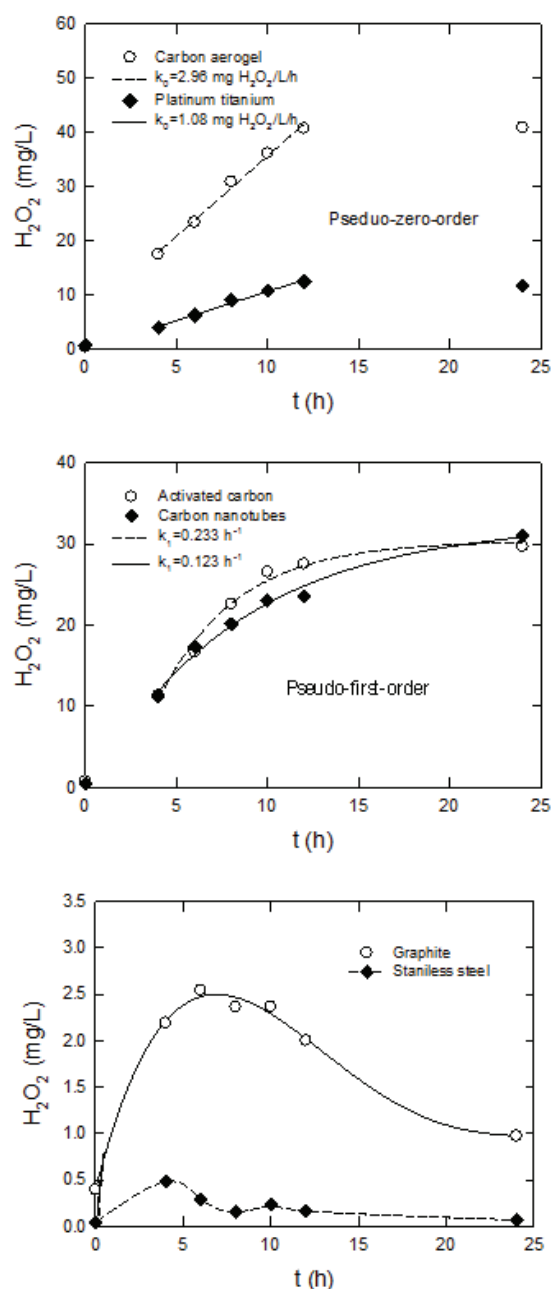


Fig. 6. Reaction kinetics of H_2O_2 for different cathode materials.

H_2O_2 production. However, increase of H_2O_2 concentrations seemed to cease close to 24 h. This is likely because of the insufficient supply of H^+ from anode biofilm. As we can see from Fig. 2, biodegradation of COD gradually slowed down from 12 to 24 h, which would result in the decreasing H^+ supply to the cathode. Therefore, even catalytic materials could not sustain high H_2O_2 production rate, and H_2O_2 concentrations would not significantly increase after 12 h.

From Fig. 6, the H_2O_2 generation rate for high specific surface area cathode materials such as activated carbons and carbon nanotubes followed pseudo-first order reaction kinetics with $r^2 = 0.9926$ and 0.9904 , respectively, showing that H_2O_2 production rate of those materials slowed

Table 1
Hydrogen peroxide production per unit area

Materials	H ₂ O ₂ mg L ⁻¹	H ₂ O ₂ mg cm ⁻²
Graphite	2.5	0.0003
Steel	0.6	0.011
Pt/Ti	9.4	0.017
Activated carbon	29	0.060
Carbon nanotubes	31	0.065
Manganese oxide/carbon aerogel	40	0.083

down between 6–12 h as the OH⁻ concentrations gradually increase. The increase of OH⁻ concentrations facilitated the H₂O₂ self-degradation reaction, which seemed to limit the increase of H₂O₂ concentrations for these cathode materials. For the cathode materials with catalytic functionality, like manganese oxide/carbon aerogel and platinum titanium, the H₂O₂ generation rates followed pseudo-zero order reaction kinetics in the first 12 h, with the $r^2=0.9931$ and 0.9928 , respectively, suggesting that the H₂O₂ generation rates of catalytic materials were fast enough to overcome the self-degradation reaction, and therefore H₂O₂ production rates could remain constant between 6–12 h when OH⁻ concentrations gradually increase.

4. Conclusions

In this study, the H₂O₂ formation reaction of various cathode materials at low voltage from MFCs was studied. The evaluated materials included the non-catalytic materials such as graphite and steel plate, the high specific surface area materials such as carbon nanotube and activated carbon, the catalytic materials such as platinum-titanium plate as well as the high specific surface area catalytic materials such as manganese oxide/carbon aerogel. The results showed that steel plate cathode could barely produce H₂O₂ in the MFCs due to the high internal resistance that resulted in the decrease of electromotive force and the cell voltage. The cathode of high specific surface area materials produced around 30 mg L⁻¹ (0.062 mg cm⁻²) H₂O₂ in the MFC, which was considerably higher than the graphite cathode (2.5 mg L⁻¹; 0.0003 mg cm⁻²) and the catalytic platinum - titanium cathode (9.8 mg L⁻¹; 0.017 mg cm⁻²). The most efficient cathode for H₂O₂ production was high surface area catalytic material of manganese oxide/carbon aerogel, which produced 40 mg L⁻¹ (0.083 mg cm⁻²) H₂O₂. In addition, H₂O₂ generation kinetics is different on different materials. The H₂O₂ generation rates for high specific surface area materials such as activated carbons and carbon nanotubes followed pseudo-first order reaction kinetics. However, for the materials with catalytic activity, like manganese oxide/carbon aerogel and platinum titanium, the H₂O₂ generation rates followed pseudo-zero order reaction kinetics in the first 12 h. Our results suggest that cathode materials with high specific surface area and catalytic activity, such as manganese oxide/carbon aerogel, will be promising for H₂O₂ production in MFCs and further development of better cathode materials will be valuable for the future application of MFCs driven electro-Fenton system.

Acknowledgement

We thank Dr. Yupo Lin for improving the writing of the manuscript. This research was supported by the Ministry of Science and Technology, Taiwan (MOST 106-2221-E-002-023-MY3 and 105-2221-E-002-009-MY3), and the National Taiwan University from Excellence Research Program - Core Consortiums (NTUCCP-107L891303) under Higher Education Sprout Project, Ministry of Education, Taiwan.

References

- [1] P.L. McCarty, J. Bae, J. Kim, Domestic wastewater treatment as a net energy producer—can this be achieved? *Environ. Sci. Technol.*, 45 (2011) 7100–7106.
- [2] H. Liu, B.E. Logan, Electricity generation using an air-cathode single chamber microbial fuel cell in the presence and absence of a proton exchange membrane, *Environ. Sci. Technol.*, 38 (2004) 4040–4046.
- [3] J.C. Biffinger, R. Ray, B.J. Little, L.A. Fitzgerald, M. Ribbens, S.E. Finkel, B.R. Ringeisen, Simultaneous analysis of physiological and electrical output changes in an operating microbial fuel cell with *Shewanella oneidensis*, *Biotechnol. Bioeng.*, 103 (2009) 524–531.
- [4] C. Feng, S.C. D.Sharma, C.-P. Yu, In *Biotechnologies and Biomimetics for Civil Engineering*, Chapter 18 Microbial Fuel Cells for Wastewater Treatment, Springer International Publishing, 2015, pp. 411–437.
- [5] I. Gajda, J. Greenman, C. Melhuish, C. Santoro, B. Li, P. Cristiani, I. Ieropoulos, Electro-osmotic-based catholyte production by microbial fuel cells for carbon capture, *Water Res.*, 86 (2015) 108–115.
- [6] I. Gajda, J. Greenman, C. Melhuish, I.A. Ieropoulos, Electricity and disinfectant production from wastewater: Microbial fuel cell as a self-powered electrolyser, *Sci. Rep.*, 6 (2016) 25571.
- [7] C.H. Feng, F.B. Li, H.J. Mai, X.Z. Li, Bio-electro-Fenton process driven by microbial fuel cell for wastewater treatment, *Environ. Sci. Technol.*, 44 (2010) 1875–1880.
- [8] Y. Wang, C. Feng, Y. Li, J. Gao, C.P. Yu, Enhancement of emerging contaminants removal using Fenton reaction driven by H₂O₂-producing microbial fuel cells, *Chem. Eng. J.*, 307 (2017) 679–686.
- [9] M. Umar, H.A. Aziz, M.S. Yusoff, Trends in the use of Fenton, electro-Fenton and photo-Fenton for the treatment of landfill leachate, *Waste Manage.*, 30 (2010) 2113–2121.
- [10] L. Fu, S.J. You, F.L. Yan, M.M. Gao, X.H. Fang, G.Q. Zhang, Synthesis of hydrogen peroxide in microbial fuel cell, *J. Chem. Technol. Biotechnol.*, 85 (2010) 715–719.
- [11] E. Rosales, M. Pazos, M.A. Longo, M.A. Sanromán, Electro-Fenton decoloration of dyes in a continuous reactor: a promising technology in colored wastewater treatment, *Chem. Eng. J.*, 155 (2009) 62–67.
- [12] U. Kurt, O. Apaydin, M.T. Gonullu, Reduction of COD in wastewater from an organized tannery industrial region by Electro-Fenton process, *J. Hazard. Mater.*, 143 (2007) 33–40.
- [13] P.V. Nidheesh, R. Gandhimathi, Trends in electro-Fenton process for water and wastewater treatment: an overview, *Desalination*, 299 (2012) 1–15.
- [14] W. Liu, Z. Ai, L. Zhang, Design of a neutral three-dimensional electro-Fenton system with foam nickel as particle electrodes for wastewater treatment, *J. Hazard. Mater.*, 243 (2012) 257–264.
- [15] X. Zhang, L. Lei, B. Xia, Y. Zhang, J. Fu, Oxidization of carbon nanotubes through hydroxyl radical induced by pulsed O₂ plasma and its application for O₂ reduction in electro-Fenton, *Electrochim. Acta*, 54 (2009) 2810–2817.
- [16] Y.H. Lin, T.Y. Wei, H.C. Chien, S.Y. Lu, Manganese oxide/carbon aerogel composite: an outstanding supercapacitor electrode material, *Adv. Energy Mater.*, 1 (2011) 901–907.
- [17] F.C. Wu, R.L. Tseng, C.C. Hu, C.C. Wang, Physical and electrochemical characterization of activated carbons prepared from firwoods for supercapacitors, *J. Power Sources*, 138 (2004) 351–359.

- [18] M. Behera, P.S. Jana, M.M. Ghangrekar, Performance evaluation of low cost microbial fuel cell fabricated using earthen pot with biotic and abiotic cathode, *Bioresource Technol.*, 101 (2010) 1183–1189.
- [19] T. Fromherz, C. Mendoza, F. Ruetter, Chemisorption of atomic H, C, N and O on a cluster-model graphite surface, *Mon. Not. R. Astron. Soc.*, 263 (1993) 851–860.
- [20] E.S. Bobkova, T.G. Shikova, V.I. Grinevich, V.V. Rybkin, Mechanism of hydrogen peroxide formation in electrolytic-cathode atmospheric-pressure direct-current discharge, *High Energy Chem.*, 46 (2012) 56–59.
- [21] T. Jacob, The mechanism of forming H_2O from H_2 and O_2 over a Pt catalyst via direct oxygen reduction, *Fuel Cells*, 6 (2006) 159–181.
- [22] C. Gao, L. Liu, T. Yu, F. Yang, Development of a novel carbon-based conductive membrane with in-situ formed MnO_2 catalyst for wastewater treatment in bio-electrochemical system (BES), *J. Membr. Sci.*, 549 (2018) 533–542.
- [23] A. Kozawa, R.A. Powers, The manganese dioxide electrode in alkaline electrolyte; the electron-proton mechanism for the discharge process from MnO_2 to $\text{MnO}_{1.5}$, *J. Electrochem. Soc.*, 113 (1966) 870–878.